

Bandwidth Efficient and Rate-Matched Low-Density Parity-Check Coded Modulation

Georg Böcherer, *Member, IEEE*, Patrick Schulte, and Fabian Steiner

Abstract—A new coded modulation scheme is proposed. At the transmitter, the concatenation of a distribution matcher and a systematic binary encoder performs probabilistic signal shaping and channel coding. At the receiver, the output of a bitwise demapper is fed to a binary decoder. No iterative demapping is performed. Rate adaption is achieved by adjusting the input distribution and the transmission power. The scheme is applied to bipolar amplitude shift keying (ASK) constellations with equidistant signal points and it is directly applicable to two-dimensional quadrature amplitude modulation (QAM). The scheme is implemented by using the DVB-S2 low-density parity-check (LDPC) codes. At a frame error rate of 10^{-3} , the new scheme operates within less than 1 dB of the AWGN capacity $\frac{1}{2} \log_2(1 + \text{SNR})$ at any spectral efficiency between 1 and 5 bits/s/Hz by using only 5 modes, i.e., 4-ASK with code rate 2/3, 8-ASK with 3/4, 16-ASK and 32-ASK with 5/6 and 64-ASK with 9/10.

I. INTRODUCTION

Reliable communication over the additive white Gaussian noise (AWGN) channel is possible if the transmission rate per real dimension does not exceed the capacity-power function

$$C(P) = \frac{1}{2} \log_2(1 + P/1) \quad (1)$$

where P is the transmission power and $P/1$ is the *signal-to-noise ratio* (SNR). An important consequence of (1) is that to achieve power and bandwidth efficient transmission over a substantial range of SNR, a communication system must adapt its transmission rate to the SNR. Contemporary standards such as DVB-S2 [1] support input constellations of different sizes and forward error correction (FEC) at various code rates. The combination of a constellation size with a code rate forms a transmission mode. By choosing the appropriate mode, the system adapts to the SNR. In Fig. 1 we display the operating points where a frame error rate (FER) less or equal to 10^{-3} can be achieved by bipolar *amplitude-shift keying* (ASK) constellations and the DVB-S2 *low-density parity-check* (LDPC) codes. Observe that the SNR gap between the operating points and the capacity-power function varies with the SNR. At the upper corner points, the gap is between 2 and 2.5 dB. Two factors contribute to this gap: first, the LDPC codes have finite length (coding gap) and second, the input

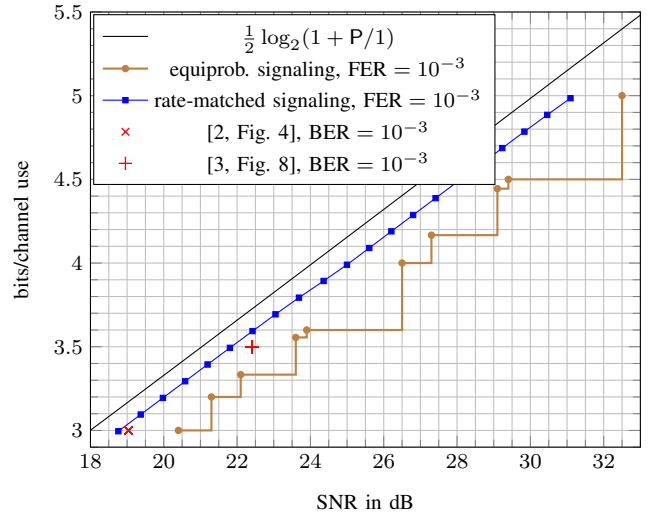


Fig. 1. Comparison of rate-matching by non-equiprobable signaling to conventional equiprobable signaling. Both schemes use LDPC codes from the DVB-S2 standard. Gains of up to 4 dB (at a spectral efficiency of 4.6 bits/s/Hz) are obtained. The rate-matched scheme uses two modes, namely 64-ASK with a rate 9/10 code and 32-ASK with a rate 5/6 code. Equiprobable signaling uses 12 modes, which combine {16, 32, 64}-ASK with {3/4, 4/5, 5/6, 8/9, 9/10} rate codes. The two schemes are evaluated at a frame error rate (FER) of 10^{-3} . For comparison, the operating points of the turbo coded modulation schemes with probabilistic shaping suggested in [2] (red \times) and [3] (red $+$) are displayed. The operating points of [2], [3] have a bit error rate (BER) of 10^{-3} . Since $\text{BER} \leq \text{FER}$, our rate-matched scheme is more energy efficient than the schemes suggested in [2], [3], see Sec. II-A for a further discussion.

distribution is uniform (shaping gap). At the lower corner points, the gap can be as large as 4.5 dB because the system resorts to one of the supported transmission modes.

To provide modes with a finer granularity, we can increase the number of code rates and constellation sizes. This approach is taken in the extension DVB-S2X [4] of DVB-S2. The system complexity increases with the number of supported code rates, which suggests the use of rate-compatible codes [5]. In [6]–[9], rate-compatible LDPC codes are designed.

In this work, we take a different approach and propose a new coded modulation scheme that uses probabilistic shaping to solve the problem of coarse mode granularity and to remove the shaping gap. With ASK constellations and only one LDPC code rate per constellation size, our scheme operates within less than 1 dB of capacity over the whole considered range of SNR, see Fig. 1. For the transmitter, we propose a new scheme, which we call *probabilistic amplitude shaping* (PAS). At the receiver, bit-metric decoding [10]–[12] is used. No iterative demapping is required. Our scheme directly applies

G. Böcherer and P. Schulte are with the Institute for Communications Engineering, Technische Universität München (TUM). F. Steiner was with the Institute for Communications Engineering, TUM. He is now with the Institute for Circuit Theory and Signal Processing, TUM.

This work was supported by the German Ministry of Education and Research in the framework of an Alexander von Humboldt Professorship. Emails: georg.boecherer@tum.de, patrick.schulte@tum.de, fabian.steiner@tum.de.

to two-dimensional *quadrature amplitude modulation* (QAM) constellations by mapping two real ASK symbols to one complex QAM symbol.

This work is organized as follows. In Sec. II, we give an overview of the related literature on coded modulation with probabilistic shaping. In Sec. III, we review the information theoretic limits of the AWGN channel and we discuss optimal signaling for ASK constellations. We introduce PAS in Sec. IV and we show in Sec. V how PAS can be implemented by distribution matching. In Sec. VI, we combine PAS at the transmitter with bit-metric decoding at the receiver. We discuss in Sec. VII the code design problem posed by our scheme and present a bit-mapper optimization heuristic. We propose a rate adaption scheme in Sec. VIII and we discuss numerical results in Sec. IX. The work is concluded in Sec. X.

II. RELATED LITERATURE

On the additive white Gaussian noise (AWGN) channel, uniformly distributed inputs can be up to 1.53 dB less power efficient than Gaussian inputs [13, Sec. IV.B], see also Sec. III-D of this work. Coded modulation with probabilistic shaping uses a non-uniform distribution on equidistant signal points to overcome the shaping gap. For works with a theoretical focus on the topic, see for example [14], [15] and references therein. Here, we review some of the existing works that address the practical implementation of probabilistic shaping.

A. Gallager's Scheme

Gallager proposes in [16, p. 208] to use a many-to-one mapping to turn a channel with non-uniform inputs into a super channel with uniform inputs. This approach is combined with turbo coding in [2] and [3]. In [17], Gallager's scheme is combined with convolutional codes. Optimal mappings are investigated in [18], see also [19, Sec. I.B]. When Gallager's scheme is combined with binary *forward error correction* (FEC), undoing the many-to-one mapping at the receiver is challenging. In [2], [3], [17], this inversion is achieved by iterative demapping, which increases the system complexity compared to uniform signaling. In [3], the authors choose the many-to-one mapping according to the desired transmission rate. The resulting rate granularity is coarse. To achieve a finer granularity, more bits must be mapped to the same signal point, which increases the system complexity further.

B. Trellis Shaping

Trellis shaping is proposed in [20] and it is discussed in detail in [21, Chap. 4] and [22, Sec. 4.4]. The transmitter first selects a set of sequences. A shaping code then selects from this set the sequence of minimum energy for transmission. The authors of [23] combine multilevel coding with trellis shaping using convolutional codes, see also [24, Sec. VIII.]. *Bit-interleaved coded modulation* (BICM) [25], [26] is used in [27] for lower bit levels and a convolutional shaping code selects the two highest bit-levels for energy minimization. LDPC codes were used as shaping codes in [28]. Since shaping is achieved by the decoder of a shaping code, it is difficult to make trellis shaping flexible to support different shaping rates.

C. Shell Mapping

Shell mapping [29] was proposed independently by several groups around the same time, see [30, Sec. VII.], [21, Chap. 8]. In shell mapping, the transmitter first selects a shell, which is a set of low energy input sequences. It then selects a sequence within the selected shell for transmission. Shell mapping combined with trellis coding is used in the ITU-T Recommendation V.34 [31]. The main challenge is to efficiently index the shells.

D. Superposition Coding

Superposition coding was proposed in [32]. The transmitter uses several encoders. Each encoder maps its output to a signal point. The selected signal points are then superposed and transmitted. The receiver uses multistage decoding. Turbo codes are considered in [32] and variations of superposition coding are proposed and analyzed in [33]. The author of [34] uses LDPC codes and proposes signal constellations that reduce the number of decoding stages. Superposition coding requires sequential decoding of the individual codes or iterative demapping.

E. Concatenated Shaping

The authors of [35] concatenate BICM encoding with shaping. A turbo encoder is followed by a one-to-one shaping block code. The scheme is improved in [36] by iterative demapping. A variation of this scheme is presented in [37], where the one-to-one shaping block code is followed by a many-to-one mapping reminiscent of Gallager's scheme. The shaping scheme [36] is used in [38] with LDPC codes on *amplitude and phase-shift keying* (APSK) constellations. Since the shaping decoder is placed before the FEC decoder, only limited gains are observed in [35]. The works [36]–[38] therefore use iterative demapping.

F. Bootstrap Scheme

A bootstrap scheme is proposed in [39], [40, Chap. 7], which separates shaping and FEC by first shaping the data and then systematically encoding the shaped data. The generated check bits are also shaped and embedded in the shaped data of the next transmission block. The bootstrap scheme is implemented in [39], [40, Chap. 7] using Geometric Huffman Coding [41] for shaping and LDPC codes from the DVB-S2 standard for FEC. Since shaping is done prior to FEC encoding, the bootstrap scheme borrows from the reverse concatenation proposed in [42], [43] for magnetic recording. The authors in [15] call the bootstrap scheme *chaining construction* and prove that it is capacity-achieving for any discrete memoryless channel. The drawback of the bootstrap scheme is that shaping is done over several consecutive transmission blocks, which have to be decoded in reverse (bootstrapped). This increases the latency and is prone to error propagation over blocks.

TABLE I
SNR GAPS IN DB OF X^\clubsuit TO UNIFORM ASK AND CAPACITY $C(P)$.

constellation	rate [bits/channel use]	X^\clubsuit	uniform ASK		capacity $C(P)$	
		SNR [dB]	SNR [dB]	gap [dB]	SNR [dB]	gap [dB]
4ASK	1	4.8180	5.1181	-0.3001	4.7712	0.0468
8ASK	2	11.8425	12.6187	-0.7761	11.7609	0.0816
16ASK	3	18.0910	19.1681	-1.0772	17.9934	0.0975
32ASK	4	24.1706	25.4140	-1.2434	24.0654	0.1052
64ASK	5	30.2078	31.5384	-1.3307	30.0988	0.1090

III. OPTIMAL SIGNALING OVER THE AWGN CHANNEL

The discrete time AWGN channel at time instance i is described by the input-output relation

$$Y_i = X_i + Z_i \quad (2)$$

where the noise terms Z_i , $i = 1, 2, 3, \dots$ are independent and identically distributed (iid) according to a zero mean Gaussian distribution with variance one. For n_c channel uses, the input is subject to the power constraint

$$\frac{\mathbb{E} [\sum_{i=1}^{n_c} |X_i|^2]}{n_c} \leq P \quad (3)$$

where $\mathbb{E}[\cdot]$ denotes expectation.

A. AWGN Capacity

Let $\hat{X}^{n_c} = \hat{X}_1, \hat{X}_2, \dots, \hat{X}_{n_c}$ be the output of the decoder that estimates the input X^{n_c} from the output Y^{n_c} . The block error probability is $P_e = \Pr(\hat{X}^{n_c} \neq X^{n_c})$. The channel coding theorem [16, Theorem 7.4.2] states that by choosing n_c large enough, P_e can be made as small as desired if the transmission rate R is smaller than the channel capacity $C(P)$. The goal of this work is to design a modulation scheme that achieves reliable transmission close to the capacity-power function (1), i.e., for **any** average signal power P , we want to reliably transmit data over the AWGN channel at a rate that is close to $C(P)$.

B. Amplitude Shift Keying

Let X be distributed on some finite alphabet \mathcal{X} of signal points and suppose $\mathbb{E}[|X|^2] = P$. The channel coding theorem states that reliable transmission at rate R with average power P is possible if

$$R < \mathbb{I}(X; Y) \quad (4)$$

where $\mathbb{I}(\cdot; \cdot)$ denotes the mutual information in bits. The first step in designing a coded modulation system is thus to choose an alphabet \mathcal{X} and a distribution P_X on \mathcal{X} such that $\mathbb{I}(X; Y)$ is close to the maximum value $C(P)$. As input alphabet, we use an ASK constellation with 2^m signal points, namely

$$\mathcal{X} = \{\pm 1, \pm 3, \dots, \pm(2^m - 1)\}. \quad (5)$$

We scale X by the *constellation scaling* $\Delta > 0$ and the resulting input/output relation is

$$Y = \Delta X + Z. \quad (6)$$

The power constraint for X is now

$$\mathbb{E}[|\Delta X|^2] \leq P. \quad (7)$$

C. Optimization of the ASK Input

We use signal point $x \in \mathcal{X}$ with probability

$$P_{X_\nu}(x) = A_\nu e^{-\nu|x|^2}, \quad A_\nu = \frac{1}{\sum_{x' \in \mathcal{X}} e^{-\nu|x'|^2}}. \quad (8)$$

The scalar A_ν ensures that the probabilities assigned by P_{X_ν} add to 1. Distributions of the form (8) are called *Maxwell-Boltzmann distributions*, see, e.g., [44]. For a fixed constellation scaling Δ and power constraint P , we choose the input distribution

$$P_{X_\Delta}(x) = P_{X_\nu}(x) \text{ with } \nu: \mathbb{E}[|\Delta X_\nu|^2] = P. \quad (9)$$

The distribution P_{X_Δ} maximizes entropy subject to the power constraint (7), see [45, Chapter 12]. Some basic manipulations show that $\mathbb{E}[|X_\nu|^2]$ is strictly monotonically decreasing in ν . Thus, the value of ν for which the condition (9) is fulfilled can be found efficiently by using the *bisection method*. For each constellation scaling Δ , the distribution P_{X_Δ} satisfies the power constraint. We now maximize the mutual information over all input distributions from this family, i.e., we solve

$$\max_{\Delta} \mathbb{I}(X_\Delta; \Delta X_\Delta + Z). \quad (10)$$

The mutual information $\mathbb{I}(X_\Delta; \Delta X_\Delta + Z)$ is a unimodal function of Δ and the optimization problem can be solved efficiently by using the *golden section method*. We denote the maximizing scaling by Δ^\clubsuit and the corresponding distribution by P_{X^\clubsuit} .

D. Shaping Gap

In Table I, we display the shaping gains of our input X^\clubsuit as compared to a uniformly distributed input. For increasing rates and constellation sizes, the shaping gain increases and approaches the upper bound of $10 \log_{10} \frac{\pi e}{6} \approx 1.53$ dB [13, Sec. IV.B]. The bound can also be derived by probabilistic arguments, see [46, Comment 4)]. For 64-ASK and a rate of 5 bits per channel use, the shaping gain is 1.33 dB.

Remark 1. *The distribution P_{X^\clubsuit} is suboptimal in general. The optimal distribution P_{X^*} can be approximated numerically by using the Blahut-Arimoto algorithm [47], [48]. However, there is no analytical expression of P_{X^*} . For the operating points in Table I, the energy efficiency of X^\clubsuit is within 0.1 dB of capacity $C(P)$, so the gain from optimizing further is bounded by 0.1 dB.*

E. Input Distribution: Operational Meaning

Suppose we use the channel n_c times, i.e., we transmit length n_c codewords. We use codeword x^{n_c} with probability $P_{X^{n_c}}(x^{n_c})$. If our transmission rate R is larger than the average mutual information between input and output, i.e., if

$$R > \frac{\sum_{i=1}^{n_c} \mathbb{I}(X_i; Y_i)}{n_c} \quad (11)$$

then the probability of error $\Pr(\hat{X}^n \neq X^n)$ is bounded away from zero for any decoder. This result follows as a corollary of the converse of the channel coding theorem [16, Theorem 7.3.1].

The mutual information terms $\mathbb{I}(X_i; Y_i)$ are calculated according to the marginal distributions P_{X_i} . We call the condition (11) the *Coded Modulation Converse*. The insight we take from (11) is that building a transmitter with marginal input distributions

$$P_{X_i} \approx P_{X^\clubsuit} \quad (12)$$

is necessary to achieve reliable transmission close to the rates displayed for X^\clubsuit in Table I.

IV. PROBABILISTIC AMPLITUDE SHAPING

We now develop a transmitter with property (12).

A. Preliminaries

We make the following two observations:

1) *Amplitude-Sign Factorization*: We can write X^\clubsuit as

$$X^\clubsuit = A \cdot S \quad (13)$$

where $A = |X^\clubsuit|$ is the *amplitude* of the input and where $S = \text{sign}(X^\clubsuit)$ is the *sign* of the input. By (5), the amplitudes take values in

$$\mathcal{A} := \{1, 3, \dots, 2^m - 1\}. \quad (14)$$

We see from (8) that the distribution P_{X^\clubsuit} is symmetric around zero, i.e., we have

$$P_{X^\clubsuit}(x) = P_{X^\clubsuit}(-x) \quad (15)$$

and therefore, A and S are stochastically independent and S is uniformly distributed, i.e., we have

$$P_{X^\clubsuit}(x) = P_A(|x|) \cdot P_S(\text{sign}(x)), \quad \forall x \in \mathcal{X} \quad (16)$$

$$P_S(1) = P_S(-1) = \frac{1}{2}. \quad (17)$$

2) *Uniform Check Bit Assumption*: The second observation is on systematic binary encoding. A systematic generator matrix of an (n, k) binary code has the form

$$\mathbf{G} = [\mathbf{I}_k | \mathbf{P}] \quad (18)$$

where \mathbf{I}_k is the $k \times k$ identity matrix and \mathbf{P} is a $k \times (n - k)$ matrix. \mathbf{P} is the *parity matrix* of the code. The generator matrix \mathbf{G} maps k data bits D^k to a length n codeword via

$$D^k \mathbf{G} = (D^k R^{n-k}) \quad (19)$$

where R^{n-k} are redundant bits that are modulo-two sums of data bits. See Fig. 2 for an illustration. The distribution of the

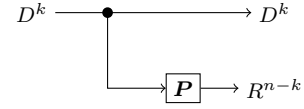


Fig. 2. Uniform check bit assumption [40, Sec. 7.1.3]: Data bits $D^k = D_1 D_2 \dots D_k$ with some arbitrary distribution P_{D^k} (the data bits are possibly dependent and non-uniformly distributed) are encoded by a systematic generator matrix $[\mathbf{I}_k | \mathbf{P}]$ of an (n, k) binary code. The encoder copies the data bits D^k to the output, which preserves the probability distribution of D^k . The encoder calculates $n - k$ redundancy bits R^{n-k} by multiplying D^k with the parity matrix \mathbf{P} . Since each R_i is a modulo two sum of several data bits, we assume that the redundancy bits R^{n-k} are approximately uniformly distributed.

modulo two sum of a large enough number of bits is close to uniform, by a central limit theorem kind of argument. The *uniform check bit assumption* [40, Sec. 7.1.3] states that the marginal distributions P_{R_i} are uniform for a large class of data distributions P_{D^k} .

B. Encoding Procedure

Consider block transmission with n_c symbols from a 2^m -ASK constellation. Since we use binary error correcting codes, we label each of the 2^{m-1} amplitudes by a binary string of length $m - 1$ and we label each of the signs ± 1 by a bit, i.e., we use

$$A \mapsto \mathbf{b}(A) \in \{0, 1\}^{m-1} \quad (20)$$

$$S \mapsto b(S) \in \{0, 1\}. \quad (21)$$

For the sign, we use $b(-1) = 0$ and $b(1) = 1$. We discuss the choice of $\mathbf{b}(A)$ in Sec. VI-C. We use a rate $k/n = (m - 1)/m$ binary code with systematic generator matrix $\mathbf{G} = [\mathbf{I}_k | \mathbf{P}]$. For block transmission with n_c channel uses, the block length of the code is $n = n_c m$ and the dimension of the code is $k = n_c(m - 1)$. The encoding procedure is displayed in Fig. 3. It works as follows.

- 1) A *discrete memoryless source* (DMS) $\boxed{P_A}$ outputs amplitudes A_1, A_2, \dots, A_{n_c} that are iid according to P_A . We explain in Sec. V how the DMS $\boxed{P_A}$ can be emulated from binary data by distribution matching.
- 2) Each amplitude A_i is represented by its label $\mathbf{b}(A_i)$.
- 3) The resulting length $(m - 1)n_c = k$ binary string is multiplied by the parity matrix \mathbf{P} to generate $n - k = n_c$ sign labels $b(S_1), b(S_2), \dots, b(S_{n_c})$.
- 4) Each sign label $b(S_i)$ is transformed into the corresponding sign S_i .
- 5) The signal $X_i = A_i \cdot S_i$ is scaled by Δ and transmitted.

We call this procedure *probabilistic amplitude shaping* (PAS). Since the signs S^{n_c} are a deterministic function of the amplitudes A^{n_c} , the input symbols X_1, X_2, \dots, X_{n_c} are correlated. Let's check if the marginal distributions P_{X_i} fulfill condition

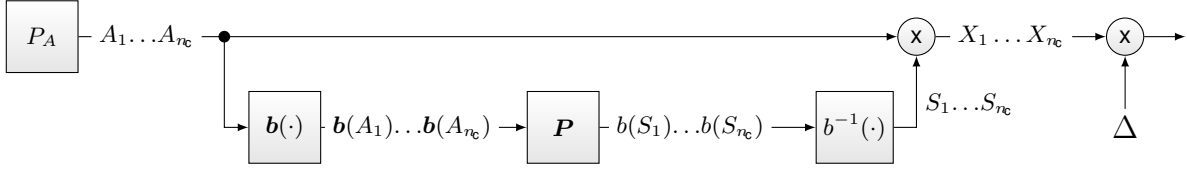


Fig. 3. PAS. The ASK amplitudes A_i take values in $\mathcal{A} = \{1, 3, \dots, 2^m - 1\}$. The amplitudes A_i are represented by their binary labels $\mathbf{b}(A_i)$. Redundancy bits $b(S_i)$ result from multiplying the binary string $b(A_1)b(A_2)\dots b(A_{n_c})$ by the parity matrix \mathbf{P} of a systematic generator matrix $[\mathbf{I}|\mathbf{P}]$. The redundancy bits $b(S_i)$ are transformed into signs S_i and multiplied with the amplitudes A_i . The resulting signal points $X_i = A_i S_i$ take values in $\mathcal{X} = \{\pm 1, \pm 3, \dots, \pm(2^m - 1)\}$. The signal points X_i are scaled by Δ and ΔX_i is transmitted over the channel.

(12). We have

$$P_{X_i}(x_i) = P_{A_i S_i}(|x_i|, \text{sign}(x_i)) \quad (22)$$

$$\approx P_{A_i}(|x_i|)P_{S_i}(\text{sign}(x_i)) \quad (23)$$

$$= P_A(|x_i|)P_{S_i}(\text{sign}(x_i)) \quad (24)$$

$$\approx P_A(|x_i|)^{\frac{1}{2}} \quad (25)$$

$$= P_{X^*}(x) \quad (26)$$

where we used the uniform check bit assumption in (25). We discuss when we have equality in (23) and (25).

- We have equality in (23) if A_i and S_i are independent. This is the case if the redundant bit $b(S_i)$ does not depend on the binary label of A_i (the bit $b(S_i)$ can still depend on other A_j , $j \neq i$). On the other hand, if $b(S_i)$ is determined by the binary index of A_i only, then A_i and S_i are dependent and we will not have equality in (23).
- Recall that $b(S_i)$ is the modulo two sum of binary random variables. If one of these binary random variables is independent of the others and uniformly distributed, then a basic probability calculation shows that $b(S_i)$ is exactly uniformly distributed and we have equality in (25).

For the rest of this work, we assume that our scheme achieves equality in (23) and (25). Our numerical results support this assumption. Of course, if the empirical results deviate from what theory predicts, we should check the assumptions of equality in (23) and (25).

Remark 2. PAS is a special case of the bootstrap scheme [15], [39]. After encoding, the redundancy bits are uniformly distributed. However, instead of transforming them into a sequence of symbols with a non-uniform distribution and transmitting them in the next block as is done in the bootstrap scheme, they can be used directly as sign labels in the same block, since the uniform distribution is already optimal.

Remark 3. PAS can be seen as a probabilistic version of shell mapping. By the weak law of large numbers,

$$\frac{\sum_{i=1}^{n_c} A_i^2}{n_c} \approx P \quad (27)$$

with high probability, i.e., the source P_A selects an amplitude sequence in a shell in the n_c -dimensional space that contains the sequences of energy $\approx n_c P$. Multiplying the amplitudes by signs does not change the power, i.e., the transmitted signal X^{n_c} remains in the shell selected by the amplitude source P_A .

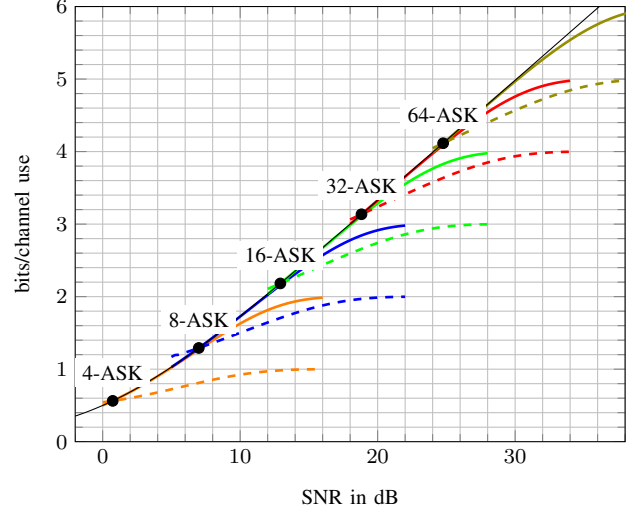


Fig. 4. The mutual information curves (solid) and the transmission rate curves (dashed) for ASK. The optimal operating points for rate $(m-1)/m$ codes are indicated by dots.

C. Optimal Operating Points

We study the rates at which reliable transmission is possible with our scheme. By (11), reliable communication at rate R is achievable only if

$$R < \frac{\sum_{i=1}^{n_c} \mathbb{I}(X_i; Y_i)}{n_c} = \mathbb{I}(X; Y) = \mathbb{I}(AS; Y). \quad (28)$$

Since A^{n_c} represents our data, our transmission rate is

$$R = \frac{\mathbb{H}(A^{n_c})}{n_c} = \mathbb{H}(A) \left[\frac{\text{bits}}{\text{channel use}} \right] \quad (29)$$

and condition (28) becomes

$$\mathbb{H}(A) < \mathbb{I}(AS; Y). \quad (30)$$

In Fig. 4, both the mutual information $\mathbb{I}(AS; Y)$ (solid lines) and transmission rate $\mathbb{H}(A)$ (dashed lines) are displayed for 4, 8, 16, 32, and 64-ASK. For high enough SNR, the mutual information saturates at m bits and the transmission rate saturates at $m-1$ bits. Optimal error correction for block length $n_c \rightarrow \infty$ would operate where the transmission rate curve crosses the mutual information curve. These crossing points are indicated by dots in Fig. 4. How to operate at other transmission rates is the topic of rate adaption and we discuss this in detail in Sec. VIII.

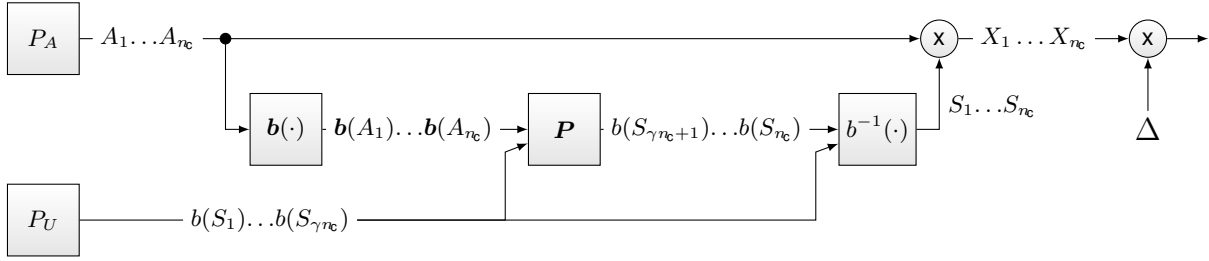


Fig. 6. Extension of PAS to code rates higher than $(m-1)/m$. The fraction γ of the signs is used for data, which is modelled as the output of a Bernoulli-1/2 DMS P_U .

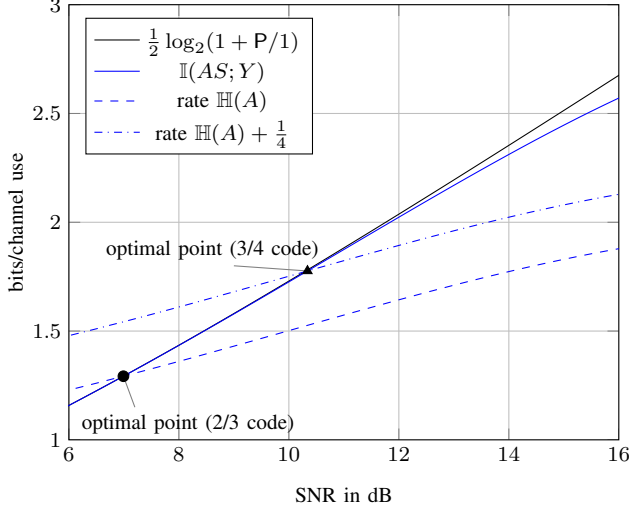


Fig. 5. Optimal operating points of 8-ASK for PAS ($c = 2/3$) and extended PAS ($c = 3/4$).

D. PAS for Higher Code Rates

We observe in Fig. 4 that the ASK mutual information curves stay close to the capacity $C(P)$ over a certain range of rates above the optimal operating points. We therefore extend our PAS scheme to enable the use of code rates higher than $(m-1)/m$ on 2^m -ASK constellations. We achieve this by using some of the signs S_i for uniformly distributed data bits. We illustrate this extension of the PAS scheme in Fig. 6. Let γ denote the fraction of signs used for data bits. We interpret γn_c uniformly distributed data bits as sign labels $b(S_1) \cdots b(S_{\gamma n_c})$. These γn_c bits and the $(m-1)n_c$ bits from the amplitude labels are encoded by the parity matrix of a rate c code, which generates the remaining $(1-\gamma)n_c$ sign labels. The code rate can be expressed in terms of m and γ as

$$c = \frac{m-1+\gamma}{m}. \quad (31)$$

For a given code rate c , the fraction γ is given by

$$\gamma = 1 - (1-c)m. \quad (32)$$

Since a fraction γ of the signs now carries information, the transmission rate of the extended PAS scheme is given by

$$R = \frac{\mathbb{H}(A^{n_c}) + \mathbb{H}(S^{\gamma n_c})}{n_c} = \mathbb{H}(A) + \gamma \left[\frac{\text{bits}}{\text{channel use}} \right]. \quad (33)$$



Fig. 7. The matcher transforms uniform data blocks of length k_c into n_c amplitudes that are approximately distributed according to the desired distribution P_A . By replacing the amplitude source P_A in the PAS diagrams in Fig. 3 and Fig. 6 by a matcher, our scheme provides a binary interface to the source coding part of a digital communication system.

The optimal operating point is then given by the crossing of the rate curve $\mathbb{H}(A) + \gamma$ and the mutual information. In Fig. 5, we display for 8-ASK the optimal operating points for $c = 2/3$ and $c = 3/4$.

V. DISTRIBUTION MATCHING

In a digital communication system, usually a binary interface separates the source coding part from the channel coding part [49, Chap. 1]. Up to now, our scheme does not have such a binary interface, since some of our data is output by an amplitude source P_A . We therefore add a device that takes as input k_c uniformly distributed independent bits U^{k_c} and outputs n_c amplitudes \tilde{A}^{n_c} . We illustrate this in Fig. 7. We require the following properties for our device:

- P1 The input provides a binary interface to the source coding part of the digital communication system.
- P2 The output is approximately the output of a DMS P_A .
- P3 The input can be recovered from the output, i.e., the mapping is invertible.

A device with such properties is called a *distribution matcher* [41]. Variable length distribution matchers were proposed in [13, Sec. IV.A], [44, Sec. VII] and [50] and their design was studied in [40], [41], [44], [51]–[53].

Variable length matchers can lead to buffer overflow, synchronization loss and error propagation, see, e.g., [44, Sec. 1]. We therefore use the fixed length distribution matcher proposed in [54]. This matcher, called *constant composition distribution matcher* (CCDM), has the properties P1 and P3. To address property P2, we need to say what we mean by “matcher output \tilde{A}^{n_c} is approximately the output of a DMS P_A ”. By [55, Theorem 1.2], a good measure for similarity in the context of channel coding is the normalized informational divergence (also known as *Kullback-Leibler divergence* or *relative entropy* [45, Sec. 2.3]) of the output distribution $P_{\tilde{A}^{n_c}}$ and the memoryless distribution $P_A^{n_c}$. The normalized

informational divergence is

$$\frac{\mathbb{D}(P_{\hat{A}^{n_c}} \| P_A^{n_c})}{n_c} = \frac{\sum_{a^{n_c} \in \text{supp } P_{\hat{A}^{n_c}}} P_{\hat{A}^{n_c}}(a^{n_c}) \log_2 \frac{P_{\hat{A}^{n_c}}(a^{n_c})}{P_A^{n_c}(a^{n_c})}}{n_c} \quad (34)$$

where $\text{supp } P_{\hat{A}^{n_c}}$ is the support of $P_{\hat{A}^{n_c}}$. The CCDM has property P2 in the following sense:

- 1) As $n_c \rightarrow \infty$, the normalized informational divergence (34) approaches zero.
- 2) As $n_c \rightarrow \infty$, the rate approaches $\mathbb{H}(A)$, i.e., we have

$$\frac{k_c}{n_c} \rightarrow \mathbb{H}(A). \quad (35)$$

We use the CCDM to emulate the amplitude source $\boxed{P_A}$. The output length n_c is finite, and we use the actual rate k_c/n_c for performance evaluations.

VI. BIT-METRIC DECODING

The receiver estimates the transmitted codeword X^{n_c} from the channel outputs Y^{n_c} . In this section, we show how this can be implemented by a bit-metric decoder.

A. Preliminaries: Binary Labeling and Decoding

Consider a coded modulation system where the input X takes values in a 2^m -ASK constellation. An optimal decoder uses the symbol-metric $p_{Y|X}$ [11, Sec. II.B] and can achieve the rate

$$R_{\text{SMD}} = \mathbb{I}(X; Y) \quad (36)$$

where SMD stands for *symbol-metric decoding* (SMD). We are interested in successfully decoding at a transmission rate close to R_{SMD} by using a *binary* decoder. Recall that our PAS scheme labels the amplitude $A = |X|$ by a length $m-1$ binary string $\mathbf{b}(A)$ and the sign $S = \text{sign}(X)$ by one bit $b(S)$. The length m binary string

$$\mathbf{B} = B_1 B_2 \cdots B_m := b(S) \mathbf{b}(A) \quad (37)$$

thus assigns to each signal point $x \in \mathcal{X}$ a label via

$$\text{label}(x) = \text{label}(\text{sign}(x)) \text{label}(|x|) = b_1 b_2 \cdots b_m. \quad (38)$$

Since the labeling is one-to-one, we can also select a signal point for transmission by choosing the label \mathbf{B} , i.e., we use

$$X = x_{\mathbf{B}} = \{x \in \mathcal{X} : \text{label}(x) = \mathbf{B}\}. \quad (39)$$

We can interpret \mathbf{B} as the channel input and the input/output relation of our channel as

$$Y = \Delta x_{\mathbf{B}} + Z. \quad (40)$$

Using the chain rule, we expand the mutual information of \mathbf{B} and Y as

$$\mathbb{I}(\mathbf{B}; Y) = \sum_{i=1}^m \mathbb{I}(B_i; Y|B^{i-1}) \quad (41)$$

$$= \mathbb{I}(B_1; Y) + \mathbb{I}(B_2; Y|B_1) + \cdots + \mathbb{I}(B_m; Y|B_1 \cdots B_{m-1}). \quad (42)$$

This expansion suggests the following binary decoding:

- 1) Use the channel output Y to calculate an estimate \hat{B}_1 .
- 2) Successively use the output Y and the estimates $\hat{B}_1 \cdots \hat{B}_{i-1}$ to calculate the next estimate \hat{B}_i .

This approach is called *multistage decoding* (MD). It requires *multilevel coding* (MLC) at the transmitter, i.e., on each bit-level, an individual binary code with block length n_c is used. MLC/MD was first introduced in [56] and it is discussed in detail, e.g., in [24]. To use MLC/MD, we would need to modify our PAS scheme. A simpler approach is to ignore the estimates \hat{B}_j , $j \neq i$ when estimating B_i . This reduces the mutual information, which can be seen as follows

$$\mathbb{I}(\mathbf{B}; Y) = \sum_{i=1}^m \mathbb{I}(B_i; Y|B^{i-1}) \quad (43)$$

$$= \sum_{i=1}^m \mathbb{H}(B_i|B^{i-1}) - \mathbb{H}(B_i|YB^{i-1}) \quad (44)$$

$$\stackrel{(a)}{\geq} \sum_{i=1}^m \mathbb{H}(B_i|B^{i-1}) - \mathbb{H}(B_i|Y) \quad (45)$$

$$\stackrel{(b)}{=} \mathbb{H}(\mathbf{B}) - \sum_{i=1}^m \mathbb{H}(B_i|Y) \quad (46)$$

where (a) follows because conditioning does not increase entropy [45, Theorem 2.6.5] and where we used the chain rule for entropy in (b). The expression in the last line of (46) can be approached as follows. We jointly encode all bit-levels by a single binary code of block length mn_c . This idea was introduced in [25] and is now usually called *bit-interleaved coded modulation* (BICM) [10], [26]. Since our PAS transmitter encodes all bit-levels by a single binary code $\mathbf{G} = [\mathbf{I}_k | \mathbf{P}]$, our transmitter is a BICM encoder. At the receiver, we use a *bit-metric decoder*.

B. Bit-Metric Decoding

A soft-demapper calculates for each bit-level i the soft-information

$$L_i = \underbrace{\log \frac{P_{B_i}(0)}{P_{B_i}(1)}}_{\text{a-priori information}} + \underbrace{\log \frac{p_{Y|B_i}(Y|0)}{p_{Y|B_i}(Y|1)}}_{\text{channel likelihood}}. \quad (47)$$

The distribution P_{B_i} and the conditional density $p_{Y|B_i}$ in (47) can be calculated as

$$P_{B_i}(b_i) = \sum_{\mathbf{a} \in \{0,1\}^m : a_i = b_i} P_{\mathbf{B}}(\mathbf{a}) \quad (48)$$

$$p_{Y|B_i}(y|b_i) = \sum_{\mathbf{a} \in \{0,1\}^m : a_i = b_i} p_{Y|\mathbf{B}}(y|\mathbf{a}) \frac{P_{\mathbf{B}}(\mathbf{a})}{P_{B_i}(b_i)}. \quad (49)$$

The soft-information L_i forms a sufficient statistic to estimate bit level B_i from the channel output Y [57, Sec. 8.2.1], i.e., we have $\mathbb{I}(B_i; Y) = \mathbb{I}(B_i; L_i)$. A bit-metric decoder uses the soft information L_1, L_2, \dots, L_m to estimate the transmitted data and achieves the rate [12, Theorem 1]

$$R_{\text{BMD}} = \mathbb{H}(\mathbf{B}) - \sum_{i=1}^m \mathbb{H}(B_i|Y). \quad (50)$$

TABLE II
TWO LABELINGS FOR THE AMPLITUDES OF 8-ASK AND THE RESULTING
SIGNAL POINT LABELINGS

		Amplitude		7	5	3	1		
natural labeling		00	01	10	11				
BRGC		00	01	11	10				
Signal point		-7	-5	-3	-1	1	3	5	7
Labeling 1		000	001	010	011	110	111	101	100
BRGC		000	001	011	010	110	111	101	100

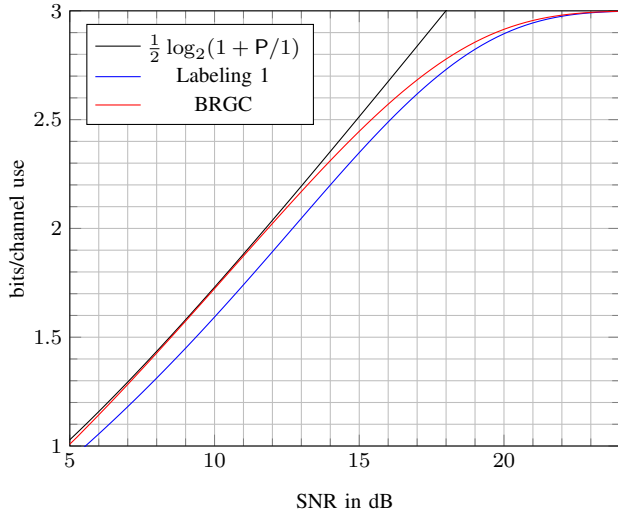


Fig. 8. Comparison of R_{BMD} for the two labelings from Table II.

Note that (50) is equal to the expression we derived in (46).

Remark 4. If the bit levels are independent, the rate becomes the “BICM capacity” [11, Theorem 1]

$$\sum_{i=1}^m \mathbb{I}(B_i; Y). \quad (51)$$

Using non-uniform distributions for the independent bit-levels results in bit-shaping, which was introduced in [58] and is discussed in [12]. The authors in [59, Eq. (1)] call (51) the “pragmatic capacity”.

From a coding perspective, bit-metric decoding transforms the channel (40) into m parallel binary input channels $p_{L_i|B_i}$, $i = 1, 2, \dots, m$.

- 1) The bit channels $p_{L_i|B_i}$ are different for different bit levels. This is important in Sec. VII, where we optimize the parity matrix \mathbf{P} for bit-metric decoding.
- 2) By (49), the distribution of the bits B_j , $j \neq i$ influences the channel transition probabilities $p_{L_i|B_i}$ of the i th bit-channel, i.e., for each bit level, the other bit-levels act as interference.
- 3) The rate (50) can take on different values for different labelings of the signal points. We discuss this next.

C. Optimizing the Labeling

We choose the labeling of the $m - 1$ amplitudes; the label of the sign is already defined by construction. We evaluate R_{BMD} for 8-ASK and two different amplitude labelings. Labeling 1

TABLE III
COMPARISON OF SNRS NEEDED BY SYMBOL-METRIC DECODING AND
BIT-METRIC DECODING TO ACHIEVE A CERTAIN RATE

constellation	rate	SNR(R_{SMD}) [dB]	SNR(R_{BMD}) [dB]	Gap [dB]
4-ASK	1	4.8180	4.8313	0.0133
8-ASK	2	11.8425	11.8481	0.0056
16-ASK	3	18.0911	18.0951	0.0039
32-ASK	4	24.1708	24.1742	0.0034
64-ASK	5	30.2078	30.2110	0.0032

is a *natural labeling* and Labeling 2 is the *Binary Reflected Gray Code* (BRGC), see [60]. The two labelings are listed in Table II. We have ordered the amplitudes in descending order so that the actual signal points are labeled from left to right. The resulting labelings of the signal points are also displayed in Table II. Note that the natural labeling of the amplitudes does not lead to a natural labeling of the signal points. In contrast, the BRGC labeling of the amplitudes also leads to the BRGC of the signal points. We display in Fig. 8 R_{BMD} for Labeling 1 and the BRGC labeling. The BRGC labeling is better than Labeling 1 and very close to the capacity $C(P)$, which is consistent with the results presented in [12]. In Table III, bit-metric decoding with BRGC is compared to symbol-metric decoding. The SNRs needed to achieve a given rate are listed.

Remark 5. The bit-metric decoding gaps in Table III show how much we can gain by using multilevel coding with multistage decoding or by iteratively exchanging extrinsic information between the soft-demapper and the soft-decoder (BICM-ID, [61]). This gain is negligible and not worth the increased complexity for the considered scenario.

VII. LDPC CODE DESIGN

In principle, our scheme works for any binary code with a systematic encoder and a decoder that can process the soft-output of the binary demappers. In this section, we discuss the deployment of LDPC codes.

A. LDPC Codes and Bit-Channels

LDPC codes are linear block codes with a sparse $(n - k) \times n$ check matrix \mathbf{H} . The matrix \mathbf{H} can be represented by a Tanner graph [62] consisting of variable nodes and check nodes. The variable node degree of the i th coded bit is given by the number of ones in the i th column of \mathbf{H} and the degree of the j th check node is given by the number of ones in the j th row of \mathbf{H} . The variable and check node degrees influence the decoding threshold of the LDPC code [63].

Good LDPC codes are often irregular, i.e., not all coded bits have the same variable node degree [63], [64]. At the same time, the coded bits are transmitted over different bit-channels. This suggests that the bit-mapper, which decides which coded bit is transmitted over which bit-channel, influences the performance. The example shown in Fig. 9 confirms this. The optimized bit-mapper is 0.6 dB more energy efficient than a randomly chosen bit-mapper.

Bit-mapper optimization was considered, e.g., in [65]–[69]. An alternative approach is to jointly optimize the node degrees

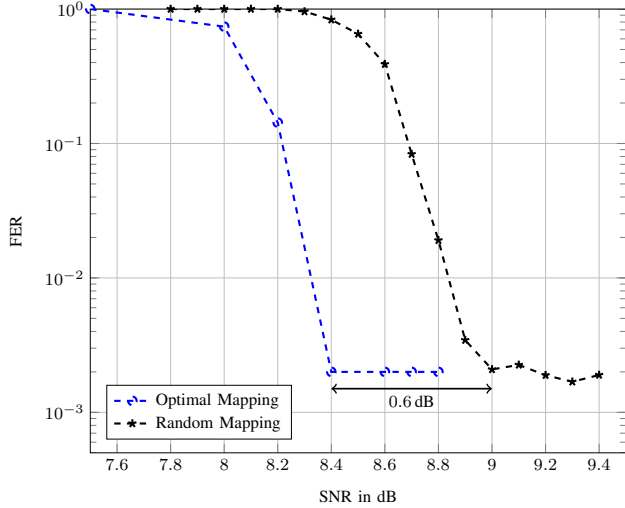


Fig. 9. Influence of the bit-mapping on the performance. The DVB-S2 rate 2/3 LDPC code is used with uniform inputs on an 8-ASK constellation. An optimized bit-mapper (blue curve) and a random bit-mapper (red curve) are used.

and the bit-mapper. This is done in [70] and [71]. In this work, we consider bit-mapper optimization.

B. Bit-Mapper Optimization for the DVB-S2 Codes

We use LDPC codes from the DVB-S2 standard. In Table IV, we display the variable node degree distributions of the DVB-S2 codes, e.g., the rate 2/3 code has 4320 coded bits of variable node degree 13, and it has 38880, 21599, and 1 bits of degrees 3, 2, and 1, respectively. All codes have four different variable node degrees, which decrease from left to right. By Sec. IV-B, our PAS scheme places the uniformly distributed bits of bit-level B_1 at the end of the codeword in the systematic encoding process. For the bit-levels $B_2 \cdots B_m$, we use the following heuristic.

- A bit interleaver π_b sorts the bit stream by bit-levels, i.e.,

$$\mathbf{b}(A_1) \dots \mathbf{b}(A_{n_c}) \xrightarrow{\pi_b} \mathbf{B}_2 \mathbf{B}_3 \cdots \mathbf{B}_m \quad (52)$$

where \mathbf{B}_i is a string of n_c bits of level i .

- A bit-level interleaver permutes the bit-level strings. We compactly represent the bit-level interleaver by listing the bit-levels in the order in which they should occur in the codeword, e.g., for $m = 4$, the bit-level interleaver (4, 2, 3) is

$$\mathbf{B}_2 \mathbf{B}_3 \mathbf{B}_4 \xrightarrow{(4,2,3)} \mathbf{B}_4 \mathbf{B}_2 \mathbf{B}_3. \quad (53)$$

We keep the bit interleaver fixed and represent the complete bit-mapping by appending a 1 to the bit-level interleaver, e.g., $\pi = (4, 2, 3, 1)$ stands for the composition of π_b with bit-level interleaver (4, 2, 3). We optimize the bit-level interleaver. There are $(m-1)!$ possibilities, among which we choose the one with the best error performance. The largest considered constellation is 64-ASK, for which we need to choose among $(6-1)! = 120$ bit level interleavers. This optimization is still feasible. We display in Table V the optimized bit-mappers for uniform inputs and rate $(m-1)/m$ codes.

TABLE IV
VARIABLE NODE DEGREE DISTRIBUTIONS OF DVB-S2 CODES

rate	variable node degrees						
	13	12	11	4	3	2	1
2/3	4320				38880	21599	1
3/4		5400			43200	16199	1
4/5			6480		45360	12959	1
5/6	5400				48600	10799	1
9/10				6480	51840	6479	1

TABLE V
OPTIMAL BIT-LEVEL INTERLEAVER FOR UNIFORM INPUTS AND DVB-S2 CODES

constellation	code rate	bit-mapper π
8ASK	2/3	(3, 2, 1)
16ASK	3/4	(3, 4, 2, 1)
32ASK	4/5	(3, 2, 5, 4, 1)
64ASK	5/6	(4, 2, 5, 3, 6, 1)

VIII. RATE ADAPTION

A. Practical Operating Points

We use PAS at the transmitter and bit-metric decoding at the receiver. The transmission rate and the achievable rate are given by the respective

$$R = \mathbb{H}(A) + \gamma, \quad R_{\text{BMD}} = \mathbb{H}(\mathbf{B}) - \sum_{i=1}^m H(B_i | L_i) \quad (54)$$

where $\mathbf{B} = b(S)b(A)$. For each transmit power P , we choose the amplitude distribution P_A and the constellation scaling Δ to maximize the achievable rate. In this way, we obtain a transmission rate curve R and an achievable rate curve R_{BMD} . In analogy to our discussion in Sec. IV-C, the optimal operating point for our scheme is where R crosses R_{BMD} . We illustrate this in Fig. 10 for 8-ASK and code rate $c = 2/3$ ($\gamma = 0$). When we use practical codes of finite block length n_c , we must back off from the optimal operating point and tolerate a positive FER. We back off along the transmission rate curve R . As we increase the transmission power P , the *rate back-off*

$$R_{\text{BMD}} - R \quad (55)$$

increases and we expect that the error probability decreases. This intuition is confirmed by the practical operating points of the 2/3 DVB-S2 LDPC code shown in Fig. 10.

B. Transmission Rate Adaption

Suppose we achieve a transmission rate R° at a FER P_e by the procedure described in Sec. VIII-A. Suppose further that this *reference operating point* is achieved by amplitude distribution P_A and constellation scaling Δ . With the same code, we now want to transmit at a rate $\tilde{R} \neq R^\circ$ and achieve the same error probability.

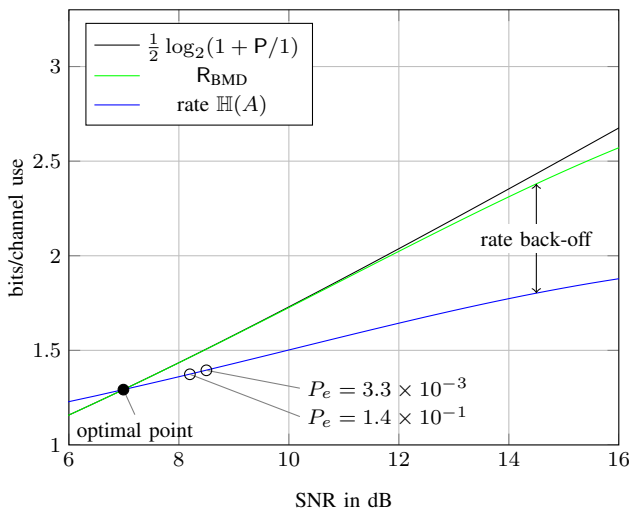


Fig. 10. Operating points for 8-ASK and rate 2/3 codes. The optimal point is where the rate curve $R(P)$ crosses the achievable rate curve $R_{\text{BMD}}(P)$. By backing off from the optimal point along the rate curve (given by the distance between the rate curve and the achievable rate curve) increases. For the rate 2/3 DVB-S2 LDPC code, the FER P_e is decreased from 1.1×10^{-1} to 2.8×10^{-3} by increasing the rate back-off.

Recall that for some optimized ν (see Sec. III-C), the input distribution P_{X^\star} is given by

$$P_{X^\star}(x) = \frac{e^{-\nu|x|^2}}{\sum_{x' \in \mathcal{X}} e^{-\nu|x'|^2}}, \quad x \in \mathcal{X}. \quad (56)$$

By (16), we can write the amplitude distribution P_A of our reference point as

$$P_A(a) = 2P_{X^\star}(a), \quad a \in \mathcal{A}. \quad (57)$$

Now define

$$P_{A^\lambda}(a) = \frac{P_A(a)e^{\lambda a^2}}{\sum_{\tilde{a} \in \mathcal{A}} P_A(\tilde{a})e^{\lambda \tilde{a}^2}}, \quad a \in \mathcal{A}. \quad (58)$$

The distribution P_{A^λ} has the following properties:

- P_A and P_{A^λ} are Maxwell-Boltzmann distributions. In particular, the set of Maxwell-Boltzmann distributions is closed under the mapping $P_A \mapsto P_{A^\lambda}$ as defined by (58).
- For $\lambda = 0$, we have $P_{A^\lambda} = P_A$.
- For $\lambda \rightarrow \nu$, P_{A^λ} approaches the uniform distribution on \mathcal{A} whose entropy is $\log_2 |\mathcal{A}| = m - 1$.
- For $\lambda \rightarrow -\infty$, P_{A^λ} approaches the distribution that chooses the smallest amplitude with probability 1. The resulting entropy is zero.

From these properties, we see that we can use P_{A^λ} to adapt the transmission rate. The range of feasible rates is

$$\gamma \leq \mathbb{H}(A^\lambda) + \gamma \leq m - 1 + \gamma. \quad (59)$$

For $\gamma = 0$, the rate is between 0 and $m - 1$. To transmit at a feasible rate R , we proceed as follows.

- Choose the amplitude distribution such that the desired transmission rate is achieved, i.e., choose

$$P_{\tilde{A}} = P_{A^\lambda} : \mathbb{H}(A^\lambda) + \gamma = \tilde{R}. \quad (60)$$

- Choose the constellation scaling $\tilde{\Delta}$ such that the resulting error probability \tilde{P}_e is the same as for the reference point, i.e., choose

$$\tilde{P}_e \stackrel{!}{=} P_e. \quad (61)$$

C. Adaption for Universal Codes

The procedure described in the previous section requires to search for the right constellation scaling Δ by repeatedly performing Monte Carlo simulations. We now show how this can be simplified significantly for universal codes. We say a code is *universal*, if P_e depends only on the rate back-off $R_{\text{BMD}} - R$. Suppose for P_A and Δ of our reference point, the achievable rate evaluates to R_{BMD}° . We can now adapt the constellation scaling as follows.

- Choose the constellation scaling $\tilde{\Delta}$ such that

$$R_{\text{BMD}}(\tilde{\Delta}, P_{\tilde{A}}) - \tilde{R} = R_{\text{BMD}}^\circ - R^\circ. \quad (62)$$

Remark 6. For PAS and bit-metric decoding, we can write the rate back-off as

$$R_{\text{BMD}} - R = 1 - \gamma - \sum_{i=1}^m H(B_i | L_i). \quad (63)$$

The term $1 - \gamma$ is constant, so P_e is determined by the sum of the conditional entropies $\sum_{i=1}^m H(B_i | L_i)$.

Remark 7. For a uniformly distributed binary input B and a rate c code, the transmission rate is $R = c$ and the achievable rate is $R^* = \mathbb{I}(B; Y)$. The rate back-off becomes

$$R^* - R = \mathbb{I}(B; Y) - c. \quad (64)$$

Since c is constant, this shows that P_e is determined by the mutual information $\mathbb{I}(X; Y)$. This property was observed for practical LDPC codes in [72].

IX. NUMERICAL RESULTS

We assess the performance of our scheme by Monte Carlo simulation. For each block, k_c uniformly distributed data bits are transmitted in n_c channel uses. γn_c of the data bits $U^k = U_1 U_2 \dots U_{k_c}$ are used for bit-level 1 (see Fig. 6). The remaining $k_c - \gamma n_c$ data bits are transformed by a CCDM matcher (see Sec. V) into a sequence of n_c amplitudes. Encoding is then done according to Fig. 6. At the receiver, bit-metric decoding is performed (see Sec. VI) and the amplitude estimates are transformed back into $k_c - \gamma n_c$ data bit estimates by a CCDM dematcher, see [54]. The dematcher output together with the other γn_c data bit estimates form the data estimate $\hat{U}^k = \hat{U}_1 \hat{U}_2 \dots \hat{U}_{k_c}$. We estimate the end-to-end FER $\text{Pr}\{\hat{U}^k \neq U^k\}$. For each FER estimate, we also provide the corresponding 95% confidence interval (CI). The spectral efficiency is $R = \frac{k_c}{n_c}$. We use the DVB-S2 LDPC codes and we decode with 100 iterations. We optimize the bit-mappers using the heuristic proposed in Sec. VII-B. For each considered (constellation, code rate) mode, we first determine the practical operating point with FER $\approx 1 \times 10^{-3}$ following the procedure

TABLE VI
64-ASK, 9/10 DVB-S2, $\pi = (4, 2, 5, 3, 6, 1)$

Rate	SNR [dB]	Gap [dB]	FER	95% CI
5.09	31.80	1.15	$4.1 \cdot 10^{-3}$	$\pm 2.1 \cdot 10^{-3}$
4.98	31.09	1.09	$8.0 \cdot 10^{-3}$	$\pm 4.0 \cdot 10^{-3}$
4.89	30.46	1.05	$6.8 \cdot 10^{-3}$	$\pm 3.4 \cdot 10^{-3}$
4.79	29.84	1.03	$7.3 \cdot 10^{-3}$	$\pm 3.7 \cdot 10^{-3}$
4.69	29.23	1.02	$6.4 \cdot 10^{-3}$	$\pm 3.2 \cdot 10^{-3}$
4.59	28.62	1.02	$3.8 \cdot 10^{-3}$	$\pm 1.9 \cdot 10^{-3}$
4.49	28.01	1.01	$6.2 \cdot 10^{-3}$	$\pm 3.1 \cdot 10^{-3}$
4.39	27.41	1.01	$7.6 \cdot 10^{-3}$	$\pm 3.8 \cdot 10^{-3}$
4.29	26.80	1.00	$9.6 \cdot 10^{-3}$	$\pm 4.8 \cdot 10^{-3}$
4.19	26.21	1.00	$1.0 \cdot 10^{-2}$	$\pm 5.1 \cdot 10^{-3}$
4.09	25.61	1.00	$1.0 \cdot 10^{-2}$	$\pm 5.1 \cdot 10^{-3}$
3.99	25.00	0.99	$1.0 \cdot 10^{-2}$	$\pm 5.0 \cdot 10^{-3}$

TABLE VII
32-ASK, 5/6 DVB-S2, $\pi = (4, 5, 2, 3, 1)$

Rate	SNR [dB]	Gap [dB]	FER	95% CI
3.62	22.60	0.82	$2.1 \cdot 10^{-3}$	$\pm 1.1 \cdot 10^{-3}$
3.99	25.09	1.07	$3.3 \cdot 10^{-3}$	$\pm 1.7 \cdot 10^{-3}$
3.89	24.36	0.94	$1.8 \cdot 10^{-3}$	$\pm 9.0 \cdot 10^{-4}$
3.79	23.69	0.87	$2.8 \cdot 10^{-3}$	$\pm 1.4 \cdot 10^{-3}$
3.69	23.05	0.84	$1.5 \cdot 10^{-3}$	$\pm 8.0 \cdot 10^{-4}$
3.59	22.42	0.82	$1.6 \cdot 10^{-3}$	$\pm 8.0 \cdot 10^{-4}$
3.49	21.80	0.81	$1.5 \cdot 10^{-3}$	$\pm 8.0 \cdot 10^{-4}$
3.39	21.19	0.80	$1.3 \cdot 10^{-3}$	$\pm 6.0 \cdot 10^{-4}$
3.29	20.58	0.80	$8.0 \cdot 10^{-4}$	$\pm 4.0 \cdot 10^{-4}$
3.19	19.98	0.80	$7.0 \cdot 10^{-4}$	$\pm 4.0 \cdot 10^{-4}$
3.10	19.37	0.80	$5.0 \cdot 10^{-4}$	$\pm 3.0 \cdot 10^{-4}$
3.00	18.76	0.80	$7.0 \cdot 10^{-4}$	$\pm 4.0 \cdot 10^{-4}$

TABLE VIII
16-ASK, 5/6 DVB-S2, $\pi = (4, 3, 2, 1)$

Rate	SNR [dB]	Gap [dB]	FER	95% CI
2.96	18.40	0.67	$2.0 \cdot 10^{-2}$	$\pm 9.8 \cdot 10^{-3}$
3.00	18.66	0.69	$3.0 \cdot 10^{-2}$	$\pm 1.4 \cdot 10^{-2}$
2.90	18.01	0.65	$2.3 \cdot 10^{-2}$	$\pm 1.2 \cdot 10^{-2}$
2.80	17.38	0.63	$2.0 \cdot 10^{-2}$	$\pm 9.8 \cdot 10^{-3}$
2.70	16.75	0.62	$1.6 \cdot 10^{-2}$	$\pm 7.8 \cdot 10^{-3}$
2.60	16.13	0.61	$1.3 \cdot 10^{-2}$	$\pm 6.7 \cdot 10^{-3}$
2.50	15.51	0.61	$7.2 \cdot 10^{-3}$	$\pm 3.6 \cdot 10^{-3}$
2.40	14.89	0.61	$3.5 \cdot 10^{-3}$	$\pm 1.8 \cdot 10^{-3}$
2.30	14.27	0.62	$2.5 \cdot 10^{-3}$	$\pm 1.3 \cdot 10^{-3}$
2.20	13.64	0.62	$1.9 \cdot 10^{-3}$	$\pm 9.0 \cdot 10^{-4}$
2.10	13.01	0.62	$1.3 \cdot 10^{-3}$	$\pm 7.0 \cdot 10^{-4}$
2.00	12.37	0.63	$5.0 \cdot 10^{-4}$	$\pm 2.0 \cdot 10^{-4}$

TABLE IX
8-ASK, 3/4 DVB-S2, $\pi = (3, 2, 1)$

Rate	SNR [dB]	Gap [dB]	FER	95% CI
1.85	11.45	0.63	$1.5 \cdot 10^{-3}$	$\pm 8.0 \cdot 10^{-4}$
2.00	12.44	0.69	$3.8 \cdot 10^{-3}$	$\pm 1.9 \cdot 10^{-3}$
1.90	11.75	0.64	$2.1 \cdot 10^{-3}$	$\pm 1.1 \cdot 10^{-3}$
1.80	11.08	0.62	$1.2 \cdot 10^{-3}$	$\pm 6.0 \cdot 10^{-4}$
1.70	10.41	0.62	$2.3 \cdot 10^{-3}$	$\pm 1.2 \cdot 10^{-3}$
1.60	9.75	0.62	$1.2 \cdot 10^{-3}$	$\pm 6.0 \cdot 10^{-4}$
1.50	9.07	0.63	$1.5 \cdot 10^{-3}$	$\pm 7.0 \cdot 10^{-4}$
1.40	8.39	0.64	$1.2 \cdot 10^{-3}$	$\pm 6.0 \cdot 10^{-4}$
1.30	7.69	0.65	$2.2 \cdot 10^{-3}$	$\pm 1.1 \cdot 10^{-3}$

TABLE X
4-ASK, 2/3 DVB-S2, $\pi = (2, 1)$

Rate	SNR [dB]	Gap [dB]	FER	95% CI
1.13	6.70	0.90	$5.2 \cdot 10^{-3}$	$\pm 2.6 \cdot 10^{-3}$
1.20	7.26	0.94	$2.6 \cdot 10^{-3}$	$\pm 1.3 \cdot 10^{-3}$
1.10	6.45	0.90	$6.4 \cdot 10^{-3}$	$\pm 3.3 \cdot 10^{-3}$
1.00	5.66	0.90	$1.4 \cdot 10^{-2}$	$\pm 6.8 \cdot 10^{-3}$

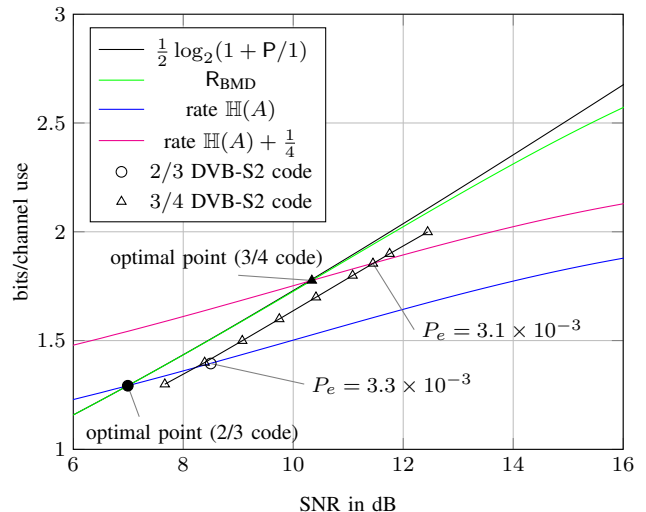


Fig. 11. Transmission rate adaption for 8-ASK. The rate 3/4 DVB-S2 code is used. The triangles mark the operating points calculated under the assumption that the code is universal. The reference operating point is the triangle on the rate $\mathbb{H}(A) + \frac{1}{4}$ curve. In Table IX, we display the FER of the adapted operating points. For comparison, we display an operating point of the 2/3 DVB-S2 code.

described in Sec. VIII-A. We then use the rate adaption (62) to operate the same (constellation, code rate) mode over a range of SNRs and spectral efficiencies. The results are displayed in Table VI–X. In the first line of each table, the practical operating point is displayed and separated from the rest of the displayed values by a horizontal line. For 8-ASK, we display the resulting operating points in Fig. 11.

1) *Spectral Efficiency*: In Table VI–X, we display the SNR gap of our scheme to capacity $C(P) = \frac{1}{2} \log_2(1 + P/1)$. Over a range of 1 bit/s/Hz to 5 bit/s/Hz, our scheme operates within 1 dB of capacity. The rate 5/6 code with 16-ASK has a gap of only 0.61 to 0.69 dB, while the rate 9/10 code with 64-ASK has a gap of 1 dB. This indicates that the spectral efficiency can be improved further by using optimized codes. The work [71] confirms this.

2) *Universality*: The results in Table VI–X show that the DVB-S2 codes are universal in the sense of Sec. VIII-C, since over the whole considered range, the resulting FER is within the waterfall region. Some configurations show a “more universal” behavior than others, e.g., the FER of the rate 3/4 code with 8-ASK (Table IX) is almost the same for the spectral efficiencies from 1.3 to 2.0 bits/s/Hz, while for the rate 5/6 code with 16-ASK, the FER changes by almost two orders of magnitude. Note that the listed operating points were found by (62). The operating points that result in a too low (too high) FER could be corrected by decreasing (increasing) the transmission power.

3) *Rate*: Since all considered codes have the same block length of 64800 bits, the number of channel uses n_c gets smaller for larger constellations. As discussed in Sec. V, the CCDDM matcher that we use to emulate the amplitude source P_A has a rate close to $\mathbb{H}(A)$ when the output length n_c is large. For the smaller constellations 4, 8 and 16-ASK, the effective rate is equal to $\mathbb{H}(A)$ with a precision of two decimal places.

For the larger constellations 32 and 64-ASK, we observe a slight decrease of the effective rate, e.g., instead of the target rate 5.00 we observe an effective rate $R = 4.98$. See also [54] for a discussion of this phenomenon. We calculate the SNR gap with respect to the effective rate.

4) *Error Floor*: The DVB-S2 codes are designed to get the FER down to a reasonable value and an outer code then lowers the error probability further [1]. Since the CCDDM dematcher performs a non-linear transformation, one corrupted symbol at the dematcher input can lead to various corrupted bit-errors at the dematcher output, so in-block error propagation can occur. In our scheme, an outer encoder should therefore be placed between the matcher and the inner encoder and the outer decoder should be placed between the inner decoder and the dematcher. To preserve the amplitude distribution imposed by the matcher, a systematic outer encoder has to be used.

X. CONCLUSIONS

We proposed a practical rate-matched coded modulation scheme that adapts its transmission rate to the SNR. At the transmitter, a distribution matcher is concatenated with a systematic encoder of a binary LDPC code. At the receiver, bit-metric decoding is used. No iterative demapping is required. The reported numerical results show that on the complex baseband AWGN channel, any spectral efficiency between 2–10 bit/s/Hz can be achieved within 1 dB of capacity $\log_2(1 + P/1)$ by using the off-the-shelf DVB-S2 LDPC codes of rate 2/3, 3/4, 4/5 and 9/10 together with QAM constellations with up to 4096 signal points. Future work should investigate rate-matched coded modulation for short block lengths and for multiple-input multiple-output channels.

REFERENCES

- [1] *Digital Video Broadcasting (DVB); 2nd Generation Framing Structure, Channel Coding and Modulation Systems for Broadcasting, Interactive Services, News Gathering and Other Broadband Satellite Applications (DVB-S2)*, European Telecommun. Standards Inst. (ETSI) Std. EN 302 307, Rev. 1.2.1, 2009.
- [2] D. Raphaeli and A. Gurevitz, "Constellation shaping for pragmatic turbo-coded modulation with high spectral efficiency," *IEEE Trans. Commun.*, vol. 52, no. 3, pp. 341–345, 2004.
- [3] M. Yankov, S. Forchhammer, K. J. Larsen, and L. P. Christensen, "Rate-adaptive constellation shaping for near-capacity achieving turbo coded BICM," in *Proc. IEEE Int. Conf. Commun. (ICC)*, 2014, pp. 2112–2117.
- [4] *Digital Video Broadcasting (DVB); Second generation framing structure, channel coding and modulation systems for Broadcasting, Interactive Services, News Gathering and other broadband satellite applications; Part 2: DVB-S2 Extensions (DVB-S2X)*, European Telecommun. Standards Inst. (ETSI) Std. EN 302 307-2, Rev. 1.1.1, 2014.
- [5] J. Hagenauer, "Rate-compatible punctured convolutional codes (RCPC codes) and their applications," *IEEE Trans. Commun.*, vol. 36, no. 4, pp. 389–400, 1988.
- [6] J. Li and K. R. Narayanan, "Rate-compatible low density parity check codes for capacity-approaching ARQ schemes in packet data communications," in *Int. Conf. Commun., Internet, Inf. Technol. (CIIT)*, 2002, pp. 201–206.
- [7] J. Ha, J. Kim, and S. W. McLaughlin, "Rate-compatible puncturing of low-density parity-check codes," *IEEE Trans. Inf. Theory*, vol. 50, no. 11, pp. 2824–2836, 2004.
- [8] T. V. Nguyen, A. Nosratinia, and D. Divsalar, "The design of rate-compatible protograph LDPC codes," *IEEE Trans. Commun.*, vol. 60, no. 10, pp. 2841–2850, 2012.
- [9] T.-Y. Chen, K. Vakili, D. Divsalar, and R. D. Wesel, "Protograph-based raptor-like LDPC codes," *IEEE Trans. Commun.*, 2015, to appear.
- [10] A. Guillén i Fàbregas, A. Martínez, and G. Caire, "Bit-interleaved coded modulation," *Found. Trends Comm. Inf. Theory*, vol. 5, no. 1–2, pp. 1–153, 2008.
- [11] A. Martínez, A. Guillén i Fàbregas, G. Caire, and F. Willems, "Bit-interleaved coded modulation revisited: A mismatched decoding perspective," *IEEE Trans. Inf. Theory*, vol. 55, no. 6, pp. 2756–2765, 2009.
- [12] G. Böcherer, "Achievable rates for shaped bit-metric decoding," *arXiv preprint*, 2015. [Online]. Available: <http://arxiv.org/abs/1410.8075>
- [13] J. Forney, G., R. Gallager, G. Lang, F. Longstaff, and S. Qureshi, "Efficient modulation for band-limited channels," *IEEE J. Sel. Areas Commun.*, vol. 2, no. 5, pp. 632–647, 1984.
- [14] C. Ling and J.-C. Belfiore, "Achieving AWGN channel capacity with lattice Gaussian coding," *IEEE Trans. Inf. Theory*, vol. 60, no. 10, pp. 5918–5929, 2014.
- [15] M. Mondelli, S. H. Hassani, and R. Urbanke, "How to achieve the capacity of asymmetric channels," in *Proc. Allerton Conf. Commun., Contr., Comput.*, 2014, pp. 789–796.
- [16] R. G. Gallager, *Information Theory and Reliable Communication*. John Wiley & Sons, Inc., 1968.
- [17] F. Schreckenbach and P. Henkel, "Signal shaping using non-unique symbol mappings," in *Proc. Allerton Conf. Commun., Contr., Comput.*, Sep. 2005.
- [18] G. Böcherer, "Optimal non-uniform mapping for probabilistic shaping," in *Proc. Int. ITG Conf. Source Channel Coding (SCC)*, 2013.
- [19] G. Böcherer and B. C. Geiger, "Optimal quantization for distribution synthesis," *arXiv preprint*, 2014. [Online]. Available: <http://arxiv.org/abs/1307.6843>
- [20] J. Forney, G. D., "Trellis shaping," *IEEE Trans. Inf. Theory*, vol. 38, no. 2, pp. 281–300, 1992.
- [21] S. A. Tretter, *Constellation Shaping, Nonlinear Precoding, and Trellis Coding for Voiceband Telephone Channel Modems with Emphasis on ITU-T Recommendation V.34*. Kluwer Academic Publishers, 2002.
- [22] R. F. H. Fischer, *Precoding and Signal Shaping for Digital Transmission*. John Wiley & Sons, Inc., 2002.
- [23] R. Fischer, J. Huber, and U. Wachsmann, "On the combination of multilevel coding and signal shaping," in *Proc. Int. ITG Conf. Source Channel Coding (SCC)*. Citeseer, 1998.
- [24] U. Wachsmann, R. F. H. Fischer, and J. B. Huber, "Multilevel codes: theoretical concepts and practical design rules," *IEEE Trans. Inf. Theory*, vol. 45, no. 5, pp. 1361–1391, 1999.
- [25] E. Zehavi, "8-PSK trellis codes for a Rayleigh channel," *IEEE Trans. Commun.*, vol. 40, no. 5, pp. 873–884, 1992.
- [26] G. Caire, G. Taricco, and E. Biglieri, "Bit-interleaved coded modulation," *IEEE Trans. Inf. Theory*, vol. 44, no. 3, pp. 927–946, 1998.
- [27] B. P. Smith and F. R. Kschischang, "A pragmatic coded modulation scheme for high-spectral-efficiency fiber-optic communications," *J. Lightw. Technol.*, vol. 30, no. 13, pp. 2047–2053, 2012.
- [28] S. Kaimalettu, A. Thangaraj, M. Bloch, and S. McLaughlin, "Constellation shaping using LDPC codes," in *Proc. IEEE Int. Symp. Inf. Theory (ISIT)*. IEEE, 2007, pp. 2366–2370.
- [29] A. K. Khandani and P. Kabal, "Shaping multidimensional signal spaces. I. optimum shaping, shell mapping," *IEEE Trans. Inf. Theory*, vol. 39, no. 6, pp. 1799–1808, 1993.
- [30] F. R. Kschischang and S. Pasupathy, "Optimal shaping properties of the truncated polydisc," *IEEE Trans. Inf. Theory*, vol. 40, no. 3, pp. 892–903, 1994.
- [31] ITU-T Recommendation V.34, "A modem operating at data signalling rates of up to 33 600 bit/s for use on the general switched telephone network and on leased point-to-point 2-wire telephone-type circuits," Feb. 1998. [Online]. Available: <http://www.itu.int/rec/T-REC-V.34-199802-I>
- [32] L. Duan, B. Rimoldi, and R. Urbanke, "Approaching the AWGN channel capacity without active shaping," in *Proc. IEEE Int. Symp. Inf. Theory (ISIT)*, 1997, p. 374.
- [33] X. Ma and L. Ping, "Coded modulation using superimposed binary codes," *IEEE Trans. Inf. Theory*, vol. 50, no. 12, pp. 3331–3343, Dec. 2004.
- [34] H. S. Cronie, "Signal shaping for bit-interleaved coded modulation on the AWGN channel," *IEEE Trans. Commun.*, vol. 58, no. 12, pp. 3428–3435, 2010.
- [35] S. Y. Le Goff, B. S. Sharif, and S. A. Jimaa, "Bit-interleaved turbo-coded modulation using shaping coding," *IEEE Commun. Lett.*, vol. 9, no. 3, pp. 246–248, 2005.
- [36] S. Y. Le Goff, B. K. Khoo, C. C. Tsimenidis, and B. S. Sharif, "Constellation shaping for bandwidth-efficient turbo-coded modulation with iterative receiver," *IEEE Trans. Wireless Commun.*, vol. 6, no. 6, pp. 2223–2233, 2007.

- [37] B. K. Khoo, S. Y. Le Goff, B. S. Sharif, and C. C. Tsimenidis, "Bit-interleaved coded modulation with iterative decoding using constellation shaping," *IEEE Trans. Commun.*, vol. 54, no. 9, pp. 1517–1520, 2006.
- [38] M. C. Valenti and X. Xiang, "Constellation shaping for bit-interleaved LDPC coded APSK," *IEEE Trans. Commun.*, vol. 60, no. 10, pp. 2960–2970, 2012.
- [39] G. Böcherer and R. Mathar, "Operating LDPC codes with zero shaping gap," in *Proc. IEEE Inf. Theory Workshop (ITW)*, 2011.
- [40] G. Böcherer, "Capacity-achieving probabilistic shaping for noisy and noiseless channels," Ph.D. dissertation, RWTH Aachen University, 2012. [Online]. Available: <http://www.georg-boecherer.de/capacityAchievingShaping.pdf>
- [41] G. Böcherer and R. Mathar, "Matching dyadic distributions to channels," in *Proc. Data Compression Conf. (DCC)*, 2011, pp. 23–32.
- [42] W. Bliss, "Circuitry for performing error correction calculations on baseband encoded data to eliminate error propagation," *IBM Tech. Discl. Bull.*, vol. 23, pp. 4633–4634, 1981.
- [43] M. Blaum, R. D. Cideciyan, E. Eleftheriou, R. Galbraith, K. Lakovic, T. Mittelholzer, T. Oenning, and B. Wilson, "High-rate modulation codes for reverse concatenation," *IEEE Trans. Magn.*, vol. 43, no. 2, pp. 740–743, 2007.
- [44] F. R. Kschischang and S. Pasupathy, "Optimal nonuniform signaling for Gaussian channels," *IEEE Trans. Inf. Theory*, vol. 39, no. 3, pp. 913–929, 1993.
- [45] T. M. Cover and J. A. Thomas, *Elements of Information Theory*, 2nd ed. John Wiley & Sons, Inc., 2006.
- [46] L. Ozarow and A. Wyner, "On the capacity of the Gaussian channel with a finite number of input levels," *Information Theory, IEEE Transactions on*, vol. 36, no. 6, pp. 1426–1428, 1990.
- [47] R. Blahut, "Computation of channel capacity and rate-distortion functions," *IEEE Trans. Inf. Theory*, vol. 18, no. 4, pp. 460–473, 1972.
- [48] S. Arimoto, "An algorithm for computing the capacity of arbitrary discrete memoryless channels," *IEEE Trans. Inf. Theory*, vol. 18, no. 1, pp. 14–20, 1972.
- [49] R. G. Gallager, *Principles of Digital Communication*. Cambridge University Press, 2008.
- [50] G. Ungerböck, "Huffman shaping," in *Codes, Graphs, and Systems*, R. Blahut and R. Koetter, Eds. Springer, 2002, ch. 17, pp. 299–313.
- [51] N. Cai, S.-W. Ho, and R. Yeung, "Probabilistic capacity and optimal coding for asynchronous channel," in *Proc. IEEE Inf. Theory Workshop (ITW)*, 2007, pp. 54–59.
- [52] R. A. Amjad and G. Böcherer, "Fixed-to-variable length distribution matching," in *Proc. IEEE Int. Symp. Inf. Theory (ISIT)*, 2013.
- [53] S. Baur and G. Böcherer, "Arithmetic distribution matching," in *Proc. Int. ITG Conf. Source Channel Coding (SCC)*, 2015.
- [54] P. Schulte and G. Böcherer, "Constant composition distribution matching," *arXiv preprint*, 2015. [Online]. Available: <http://arxiv.org/abs/1503.05133>
- [55] A. D. Wyner, "The common information of two dependent random variables," *IEEE Trans. Inf. Theory*, vol. 21, no. 2, pp. 163–179, 1975.
- [56] H. Imai and S. Hirakawa, "A new multilevel coding method using error-correcting codes," *IEEE Trans. Inf. Theory*, vol. 23, no. 3, pp. 371–377, May 1977.
- [57] R. G. Gallager, *Stochastic processes: theory for applications*. Cambridge University Press, 2013.
- [58] A. G. i Fàbregas and A. Martínez, "Bit-interleaved coded modulation with shaping," in *Proc. IEEE Inf. Theory Workshop (ITW)*, 2010, pp. 1–5.
- [59] F. Kayhan and G. Montorsi, "Constellation design for transmission over nonlinear satellite channels," in *Proc. IEEE Global Telecommun. Conf. (GLOBECOM)*, 2012, pp. 3401–3406.
- [60] F. Gray, "Pulse code communication," U. S. Patent 2632058, 1953.
- [61] X. Li and J. A. Ritcey, "Bit-interleaved coded modulation with iterative decoding," *IEEE Commun. Lett.*, vol. 1, no. 6, pp. 169–171, 1997.
- [62] R. M. Tanner, "A recursive approach to low complexity codes," *IEEE Trans. Inf. Theory*, vol. 27, no. 5, pp. 533–547, 1981.
- [63] T. J. Richardson, M. A. Shokrollahi, and R. L. Urbanke, "Design of capacity-approaching irregular low-density parity-check codes," *IEEE Trans. Inf. Theory*, vol. 47, no. 2, pp. 619–637, 1997.
- [64] M. G. Luby, M. Mitzenmacher, M. A. Shokrollahi, and D. A. Spielman, "Improved low-density parity-check codes using irregular graphs," *IEEE Trans. Inf. Theory*, vol. 47, no. 2, pp. 585–598, 2001.
- [65] Y. Li and W. E. Ryan, "Bit-reliability mapping in LDPC-coded modulation systems," *IEEE Commun. Lett.*, vol. 9, no. 1, pp. 1–3, 2005.
- [66] J. Lei and W. Gao, "Matching graph connectivity of LDPC codes to high-order modulation by bit interleaving," in *Proc. Allerton Conf. Commun., Contr., Comput.*, Sept 2008, pp. 1059–1064.
- [67] L. Gong, L. Gui, B. Liu, B. Rong, Y. Xu, Y. Wu, and W. Zhang, "Improve the performance of LDPC coded QAM by selective bit mapping in terrestrial broadcasting system," *IEEE Trans. Broadcast.*, vol. 57, no. 2, pp. 263–269, 2011.
- [68] T. Cheng, K. Peng, J. Song, and K. Yan, "EXIT-aided bit mapping design for LDPC coded modulation with APSK constellations," *IEEE Commun. Lett.*, vol. 16, no. 6, pp. 777–780, 2012.
- [69] C. Häger, A. Graell i Amat, A. Alvarado, F. Brännström, and E. Agrell, "Optimized bit mappings for spatially coupled LDPC codes over parallel binary erasure channels," in *Proc. IEEE Int. Conf. Commun. (ICC)*, Jun. 2014, pp. 2064–2069.
- [70] L. Zhang and F. Kschischang, "Multi-edge-type low-density parity-check codes for bandwidth-efficient modulation," *IEEE Trans. Commun.*, vol. 61, no. 1, pp. 43–52, January 2013.
- [71] F. Steiner, G. Böcherer, and G. Liva, "Protograph-based LDPC code design for bit-metric decoding," in *IEEE Int. Symp. Inf. Theory (ISIT)*, 2015. [Online]. Available: <http://arxiv.org/abs/1501.05595>
- [72] M. Franceschini, G. Ferrari, and R. Raheli, "Does the performance of LDPC codes depend on the channel?" *IEEE Trans. Commun.*, vol. 54, no. 12, pp. 2129–2132, 2006.